Chinese Journal of
POLYMER SCIENCE

RESEARCH ARTICLE

https://doi.org/10.1007/s10118-026-3821-4
Chinese J. Polym. Sci.

Stimuli-responsive Perovskite Hybrid Films towards Multi-mode and Dual-key Multi-level Information Encryption

Cong-Yang Ye†, Ze-Yu Feng†, Jia-He Li, Di Wang, Xiang-Xiang Xu, Yi-Fan Xie*, Hong-Li Zhang*, and Gang Zou*

State Key Laboratory of Precision and Intelligent Chemistry, Department of Polymer Science and Engineering, School of Chemistry and Materials Science, University of Science and Technology of China, Hefei 230026, China

Electronic Supplementary Information

Abstract The development of multi-mode and multi-level optical anti-counterfeiting systems holds tremendous significance for advanced information encryption and modern security. Herein, we developed a high-level information encryption platform based on a stimuli-responsive perovskite/polydiacetylene (PDA)/poly(vinyl alcohol) (PVA) composite hybrid film. By strategically integrating luminescent perovskite nanocrystals onto a twisted-stacking uniaxially oriented PDA/PVA heterostructure, three distinct optical dimensions, including pattern morphology, bright photoluminescence, and high-performance circularly polarized luminescence (CPL, with g_{lum} up to 1.0), were successfully coupled into a single flexible platform. Crucially, the three diverse optical channels can be operated independently without mutual interference. By leveraging the fast halogen anion exchange of the perovskite layer and the thermochromic phase transition of the PDA layer as orthogonal cryptographic keys, precise and reversible modulation of each optical mode was achieved. This dual-stimulus response mechanism enables a dynamic, multi-stage decryption profile that successfully transitions from a predefined camouflage state to authentic target information. This programmable and flexible hybrid film provides an innovative crosstalk-free paradigm for next-generation anti-counterfeiting and hierarchical information encryption.

Keywords Stimuli-responsive materials; Circularly polarized luminescent; Multi-modal information encryption; Twisted-stacking hierarchical structures

Citation: Ye, C. Y.; Feng, Z. Y.; Li, J. H.; Wang, D.; Xu, X. X.; Xie, Y. F.; Zhang, H. L.; Zou, G. Stimuli-responsive perovskite hybrid films towards multi-mode and dual-key multi-level information encryption. *Chinese J. Polym. Sci.* https://doi.org/10.1007/s10118-026-3821-4

INTRODUCTION

Information storage and security are becoming core issues in modern society.[1–5] Anti-counterfeiting technologies based on a single optical channel are no longer sufficient to counter escalating threats of forgery and information theft. Traditional information encryption strategies predominantly rely on single-mode optical signals such as conventional fluorescence or color changes, rendering them highly vulnerable to sophisticated counterfeiting techniques.[6,7] Multimodal optical combinations involving structural color,[8] fluorescence,[9] and colored patterns have emerged as critical methodologies for expanding the information capacity and elevating security thresholds, thereby attracting intense research interest.[10,11] In particular, the orthogonal and independent manipulation of multimodal optical signals is essential for constructing high-level crosstalk-free information encryption systems.[12–15] Recently, stimuli-responsive polymers have enabled dual-mode dynamic displays featuring both structural color and fluorescence.[16,17] Recently, circularly polarized luminescence (CPL) has attracted widespread research attention because its inherent handedness adds an exclusive high-security cryptographic dimension.[18–20] For instance, Feng *et al.* successfully constructed a multi-dimensional chiroptical film combining structural color, fluorescence, and CPL to achieve multimodal chiroptical encryption.[21] Recent advancements in multi-level encryption have demonstrated remarkable progress in increasing information density and security. The current strategies primarily focus on synergizing stimuli-responsive materials with complex photonic structures. Multi-stimulus responsiveness has been heavily exploited; for example, Wang *et al.* and Sun *et al.* utilized polymer-stabilized cholesteric liquid crystals doped with responsive elements to reveal multiple independent encrypted layers under various triggers, including visible/UV/NIR light and electric biases.[22,23] Furthermore, orthogonal decoupling of optical dimensions has driven the development of nested encryption. Pioneering works have achieved compartmentalized multiplexing by decoupling the wavelength, polarization, and spatial channels,[24] or by combining structural color patterns with touch-responsive vec-

* Corresponding authors, E-mail: yfxie@ustc.edu.cn (Y.F.X.)
E-mail: zhl1992@ustc.edu.cn (H.L.Z.)
E-mail: gangzou@ustc.edu.cn (G.Z.)
† These authors contributed equally to this work.
Special Topic: Chirality in Polymers
Received May 29, 2026; Accepted July 20, 2026; Published online September 4, 2026

tor holograms.[25] These collective efforts highlight a distinct trend toward high-dimensional dynamically switchable encryption platforms. Despite substantial progress in multi-dimensional information encryption strategies, achieving completely decoupled regulation dynamic decryption across pattern morphology, fluorescence emission, and CPL signals simultaneously still faces difficulties, as conventional multimodal systems generally suffer from severe inter-channel crosstalk, poor independent tunability, low CPL dissymmetry factors (g_{lum}), and limited stimulus responsiveness.

Beyond the integration of multi-mode signals, advancing the defensive architecture from single-level to multi-level anti-counterfeiting represents another frontier in information security.[26–28] To achieve such multi-level architectures, the deployment of dynamically tunable chiroptical systems has emerged as an elegant strategy because their optical information can serve as responsive and multi-stage cryptographic indicators to establish distinct information hierarchies. For instance, Giuseppone *et al.* realized the reversible modulation of the CPL wavelength and handedness using thermo-responsive chiral systems.[29] Ma *et al.* achieved multicolor CPL and multi-dimensional encoding *via* supramolecular gel assembly.[30] Although numerous multi-level systems have been reported, the vast majority undergo only primary-level transitions or sequential responses triggered by a single external stimulus.[31,32] This fundamentally reliance on a single cryptographic key strictly limits both the information storage capacity and the security threshold, as the encryption protocol can be readily deciphered once the single mechanism is breached, severely restricting their practical applications in high-end encryption scenarios. The rational integration of various stimulus-responsive functionalities to fabricate multi-dimensional optical systems with orthogonal response behaviors will provide an ideal paradigm for the design and development of hierarchical encryption and anti-counterfeiting systems. Perovskite nanocrystals, which are characterized by high photoluminescence quantum yields (PLQYs), tunable emission wavelengths, and programmable patterning capabilities, are excellent candidates.[33,34] Concurrently, polydiacetylene (PDA) exhibits stimuli-responsive chromism behavior, which endows twisted-stacked PDA/poly(vinyl alcohol) (PVA) heterostructures with tunable optical activity and a large asymmetric factor.[35,36] Collectively, these results are favorable for constructing multimodal and dual-key multi-level optical systems. However, the practical implementation of truly independent, reversible, and multi-level decryption of patterned, fluorescence, and CPL information still faces considerable challenges in material design.[37–40]

To address these challenges, we designed and fabricated perovskite/PDA/PVA composite hybrid films. By constructing twisting and stacking of highly oriented PDA and PVA, the system exhibits stimuli-responsive fluorescence and CPL signals with high dissymmetry factors. More importantly, by leveraging the thermochromic transition of PDA and halogen anion exchange of perovskites, each optical channel can be independently regulated, achieving orthogonal, interference-free outputs of structural color, fluorescence, and CPL, enabling a dual-key-based multi-level information encryption model. Furthermore, the composite material demonstrated excellent compatibility with flexible device integration. This work provides a robust paradigm for developing multimodal, multi-level, and dynamically programmable advanced encryption materials with significant implications for advancing information security technologies.

METHODS

Materials

Cyclopentanone (>99.0%) and octadecene (90%) were obtained from Sigma-Aldrich (St. Louis, MO, USA). Tert-butanol (≥ 99.5%), oleic acid (OA, ≥99.5%), and all other solvents were purchased from Sinopharm Chemical Reagent Co., Ltd. Cesium carbonate (Cs_2CO_3, 99.9%), lead chloride ($PbCl_2$, 99.99%), lead bromide ($PbBr_2$, 99%), lead iodide (PbI_2, 99.9%) and 9-Octadecenylamine (oleylamine, 80%–90%) were obtained from Aladdin. 10,12-Pentacosadiynoic acid (DA) was obtained from Tokyo Chemical Industry Co., Ltd. and purified by dissolution in cyclopentanone, followed by membrane filtration prior to use. PVA films with a thickness of approximately 48 μm and saponification degree of approximately 99 mol% were provided by New Blue Sky Material Industry Co., Ltd. All reagents and solvents were utilized as received without further purification.

Synthesis of $CsPbX_3$ (X = Cl, Br, I) Nanocrystals

A mixture of Cs_2CO_3 (810 mg), 1-octadecene (40 mL), and oleic acid (2.5 mL) was dehydrated at 120 °C for 1 h followed by heating at 150 °C for 1 h under N_2 protection. Lead halide powders (1.88 mmol), including PbI_2 (870 mg), $PbBr_2$ (690 mg), and $PbCl_2$ (520 mg), were dried under vacuum at 120 °C for 1 h. Subsequently, 50 mL of ODE, 5 mL of oleylamine, and 5 mL of oleic acid were added to the reaction system at 120 °C under N_2 protection. When the lead halide salts were completely dissolved, the reaction temperature was raised to 170 °C and the Cs-oleate solution (4 mL, 0.125 mol/L in ODE) was rapidly injected into the mixture. The reaction system was immediately cooled in an ice-water bath after 5 s. Finally, the resultant mixture was quenched and centrifuged, and the obtained precipitate was redispersed in n-hexane to obtain the perovskite nanocrystals.

Fabrication of Highly Oriented PDA Films

A 3 cm × 5 cm glass substrate was immersed in DA solution (cyclopentanone, 25 mg/mL) and slowly lifted to form highly oriented DA assemblies. Cyclopentanone was gradually evaporated at the liquid-substrate interface. Highly oriented anisotropic PDA films were successfully fabricated *via* ultraviolet irradiation (254 nm) through a photomask for 1 min.

Fabrication of Perovskite Fluorescent Layers

Initially, 200 mg of $CsPbX_3$ nanocrystals solution (*n*-hexane, 40 mg/mL) was incorporated into 400 mg of Sylgard 184 component B (curing agent) under continuous stirring. The mixture was vacuum-treated at room temperature for 1 h to remove residual solvent, followed by the addition of 3.60 g of Sylgard 184 component A (silicone elastomer prepolymer). The resulting homogeneous mixture was drop-cast onto a glass substrate and thermally cured at 70 °C for 3 h to obtain flexible fluorescent PDMS layers. Customized fluorescent patterns (*e.g.*, butterfly patterns) can be fabricated on flexible PET substrates *via* a screen-printing technique.

The as-prepared green perovskite quantum dot/PDMS

composite films were immersed in a mixed solution of 37 wt% hydrochloric acid (HCl) and 45 wt% hydroiodic acid (HI) under continuous stirring. The films were removed every 15 min, rinsed thoroughly with deionized water, and their fluorescence peak positions characterized. After the fluorescence peaks were fully shifted to blue or red, the films were immersed in 40 wt% HBr solution following the same procedure until the green fluorescence was recovered, which was counted as one complete cycle. The experimental results revealed that the fluorescence intensity gradually declined with increasing cycles and nearly vanished after only one cycle.

Fabrication of Twisted-stacking CPL Films

Perovskite fluorescent films were adopted as the bottom layer and assembled with PDA intermediate layers to fabricate the polarized fluorescent layers. Subsequently, a uniaxially oriented PVA film was overlaid at a twist angle of 45° to construct twisted-stacked hierarchical CPL-active structures. To fabricate bilayer heterostructures with precisely tunable interlayer azimuthal twist angles, well-aligned diacetylene monomers were first subjected to UV polymerization to produce highly oriented blue-phase PDA films. A thin layer of transparent UV-curable optical adhesive was uniformly coated on the PDA substrate. Commercially prestretched PVA films were manually rotated by a fixed in-plane azimuthal angle of 45° in either the clockwise (CW) or counterclockwise (CCW) direction, followed by conformal flat lamination on top of the PDA layer. Subsequent irradiation with 365 nm UV light for 5 min at ambient temperature fully crosslinked and cured the liquid adhesive, permanently fixing the pre-designed 45° clockwise or counterclockwise twisted stacking configuration between the top-oriented PVA overlayer and underlying PDA film.

Characterizations

UV-Vis spectra were recorded using a Shimadzu UV-2700 spectrophotometer. Circular dichroism (CD) spectra were obtained using a JASCO J-1500 spectropolarimeter. Fluorescence spectra were acquired on a Shimadzu RF-6000 fluorescence spectrometer and circularly polarized luminescence (CPL) spectra were recorded using a JASCO CPL-300 spectrometer. Transmission electron microscopy (TEM) images were recorded using a JEOL-2000.

RESULTS AND DISCUSSION

Designing Strategy

Inspired by twisted-stacking chiral architectures, a multi-mode and multi-level CPL information encryption system comprising a tunable perovskite fluorescent layer, oriented PDA polarizing layer, and stretched PVA was rationally designed (Fig. 1a). First, a color-tunable perovskite fluorescent layer was patterned onto flexible PET substrates *via* screen-printing. An oriented PDA polarizing layer was subsequently transferred onto the surface of the perovskite fluorescent layer using a Meniscus-assisted Coating method, yielding a highly polarized fluorescent film. Thereafter, a transparent oriented PVA layer acting as a phase retarder was overlaid on the aforementioned polarized fluorescent layer in twisted stacking with a 45° twist angle (either clockwise or counterclockwise), which endows the system with dynamically tunable CPL performance. Orthogonal optical modulation of the CPL signal was achieved using two independent external stimuli. Specifically, halide anion exchange can regulate the emission wavelength of the perovskite layer, thereby directly tuning the corresponding CPL. In addition, thermal treatment triggers a thermochromic phase transition within the PDA layer, which selectively modulates the CPL intensity. Notably, under unpolarized ultraviolet irradiation, distinct optical patterns can be distinguished using left- and right-handed circular polarizing filters (CPF), as illustrated in Fig. 1(a). This architecture enables multimodal information encryption by successfully decoupling the three orthogonal optical channels. Under ultraviolet (UV) excitation, independent cryptographic information can be extracted from pattern morphology, fluorescence emission, and CPL signal channels, yielding a comprehensive multi-dimensional encryption platform (Fig. 1b). Furthermore, dynamic hierarchical encryption was realized through a sequential dual-stimulus decryption protocol. The original composite film exhibited an ambiguous intermediate state with blurred or deceptive information. The layer-by-layer decryption of accurate information can only be accomplished *via* successive hydrogen iodide (HI) treatment and thermal heating, thereby establishing a high-security multi-level hierarchical encryption model (Fig. 1c). The tensile strain (%) was defined as $((L - L_0)/L_0) \times 100$, where L_0 denotes the original gauge length and L represents the length of the stretched sample. We define the tensile strain of PVA as follows: PVA films with a tensile strain of 0 correspond to non-stretched PVA, and PVA films with tensile strain values greater than 0 are defined as stretched PVA.

Generation and Modulation of CPL

The development of CPL-active materials that simultaneously integrate high chiroptical performance, excellent mechanical deformability, and tailor-made emission characteristics for multi-level information encryption applications remains a considerable challenge. Fortunately, twisted-stacked heterostructures can function as highly efficient circular polarization-selective optical filters to achieve high-performance CPL from unpolarized fluorescence, where achiral perovskite nanocrystals provide bright unpolarized fluorescence emission. Three types of $CsPbX_3$ (X = Cl, Br, I) perovskite nanocrystals (Fig. S1 in the electronic supplementary information, ESI) were employed to generate blue, green, and red emissions, respectively (Fig. S2 in ESI). For such twisted-stacking heterostructures, the degree of linear polarization of the underlying layer is a pivotal factor that determines the overall chiroptical performance. Thus Meniscus-Assisted Coating method was adopted to fabricate highly oriented PDA films. During solvent evaporation, highly aligned diacetylene (DA) monomers were formed (Fig. S3 in ESI). After ultraviolet (UV) irradiation at 254 nm for 1 min, the colorless pristine DA films turned blue, displaying prominent characteristic absorption maxima at approximately 590 and 645 nm (Fig. S4 in ESI). When subjected to polarized UV-Vis absorption characterization, strong absorbance was observed when the polarization direction of the incident light was perpendicular to the orientation direction of the hybrid film, whereas parallel polarization resulted in weaker absorbance (Fig. S5 in ESI). Polarized optical microscopy (POM) images of PDA captured at polarization angles of 0° and 90° revealed prominent absorption differences in the parallel and perpendicular directions. (Fig. S6 in ESI) Furthermore, the polarization absorption of PDA was characterized (Fig. S5 in ESI), and the calculated polarization ratio reached 10.4,

https://doi.org/10.1007/s10118-026-3821-4

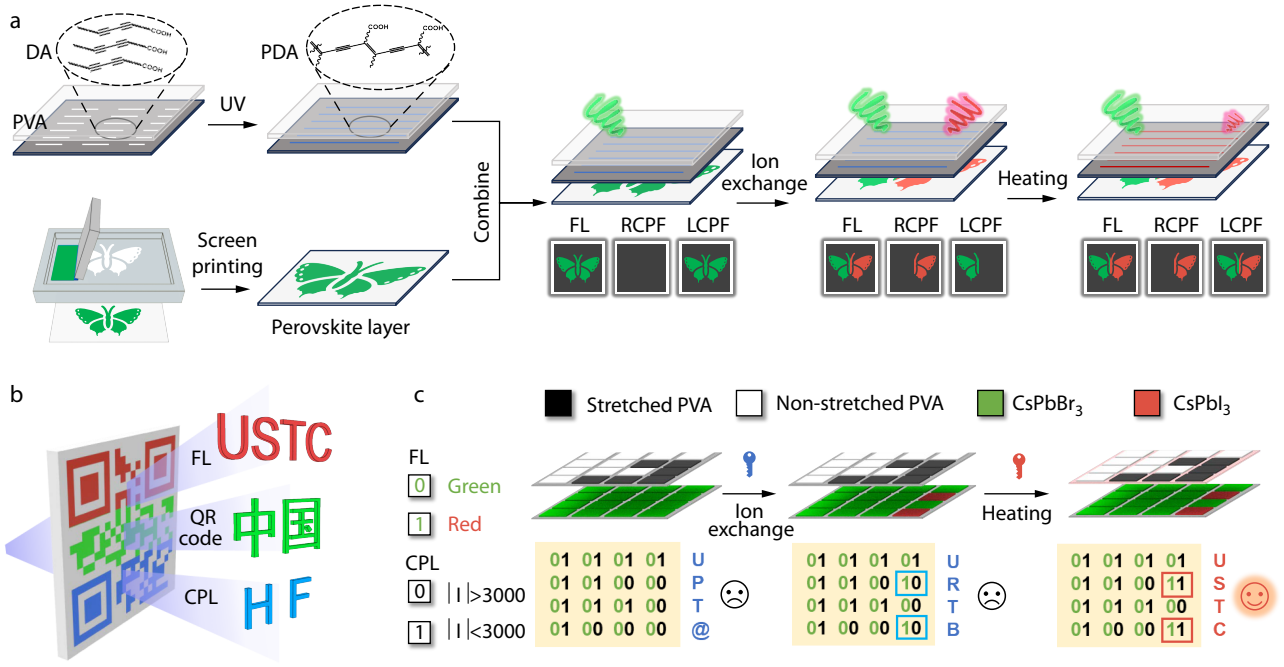

Fig. 1 Schematic diagram of preparation process, stimulus-responsive properties and multi-level multimodal encryption of twisted stacked CPL-active films. (a) Fabrication of stimulus-responsive CPL-active films; (b) Multimodal information encryption *via* orthogonal optical channels; (c) Dynamic hierarchical encryption regulated by dual stimuli.

which verified the highly ordered orientation of PDA. This phenomenon confirms the successful formation of conjugated PDA molecular backbones. As expected, overlaying one highly oriented PDA layer onto the PVA layer with a twist angle of +45° or −45° yielded a remarkable optical activity (Fig. S7 in ESI).

The intensity and handedness of the generated CPL signals are highly dependent on the configuration of the twisted-stacking heterostructures. For $CsPbCl_3$ perovskite quantum dots, the CPL intensity reaches its maximum when the twisted stacking angle between PVA and PDA ranges from 45° (Fig. S8 in ESI), which is consistent with the conclusions reported in previous work.[41,42] When the twisted stacking angle is fixed at 45°, the CPL signal evolves from near zero to a negative value, and then recovers close to zero as the tensile strain ε increases from 0% to 100%. As stretching further proceeds (ε=150%–250%), the CPL switches to a positive intensity, which first rises to a maximum and then decays. The peak value of the CPL exhibited an S-shaped variation trend as the tensile strain increased. (Fig. S9 in ESI) For example, $CsPbBr_3$ films exhibit positive CPL signals when integrated with heterostructures with a +45° stacking angle, whereas heterostructures with a −45° stacking angle generate negative CPL signals (Fig. 2a). In addition, the magnitude of the CPL signals can be modulated by varying the stacking angles, with the maximum positive and negative CPL intensities achieved at +45° and −45°, respectively. Therefore, the CPL signals of the composite system could be conveniently and precisely tailored in both handedness (from negative to positive) and intensity (from weak to strong) by adjusting the relative twist angle, with the maximum luminescence asymmetry factor (g_{lum}) reaching ±1. The spectral overlap between the unpolarized fluorescence emission of perovskite nanocrystals and the circular dichroism (CD) hands of twisted-stacked heterostructures enables the generation of blue, green, and red CPL emissions with distinct handedness. Specifically, a +45° twisted stacking structure coupled with $CsPbI_3$ nanocrystals produced negative CPL signals in the 600–800 nm spectral range (Fig. 2b). In contrast, the $CsPbCl_3$ nanocrystals exhibited positive CPL signals at 400–480 nm under 365 nm UV excitation. The opposite chiroptical responses of the twisted-stacking heterostructure in the blue and red wavelength regions stem from wavelength-dependent circular polarization selectivity toward unpolarized fluorescence at different wavelengths. These results further verify that the CPL performance of the composite films could be dynamically regulated across the visible spectrum by modulating the fluorescence emission wavelength of the perovskite nanocrystals.

Interestingly, the polymerization degree of diacetylene (DA) monomers could be systematically modulated by adjusting the UV exposure duration, which induced gradient variations in both the CD intensity and UV-Vis absorbance (Fig. S10 in ESI). This strategy enables convenient regulation of the resulting CPL signal intensity. As illustrated in Fig. 2(c), the CPL signal intensity at 500 nm exhibited a distinct positive correlation with UV irradiation time. When the irradiation duration increased from 10 s to 60 s, the corresponding CPL intensity gradually increased from approximately 0 mdeg to 850 mdeg, confirming that the PDA/PVA twisted structures could act as efficient circular polarization-selective optical filters to determine the final CPL of the system. Before stacking, all perovskite and PDA layers were prepared using identical fabrication procedures. At a fixed test voltage, the CPL signal intensity gradually increased as the number of stacked perovskite layers increased (Fig. S11a in ESI). Similarly, the CPL intensity

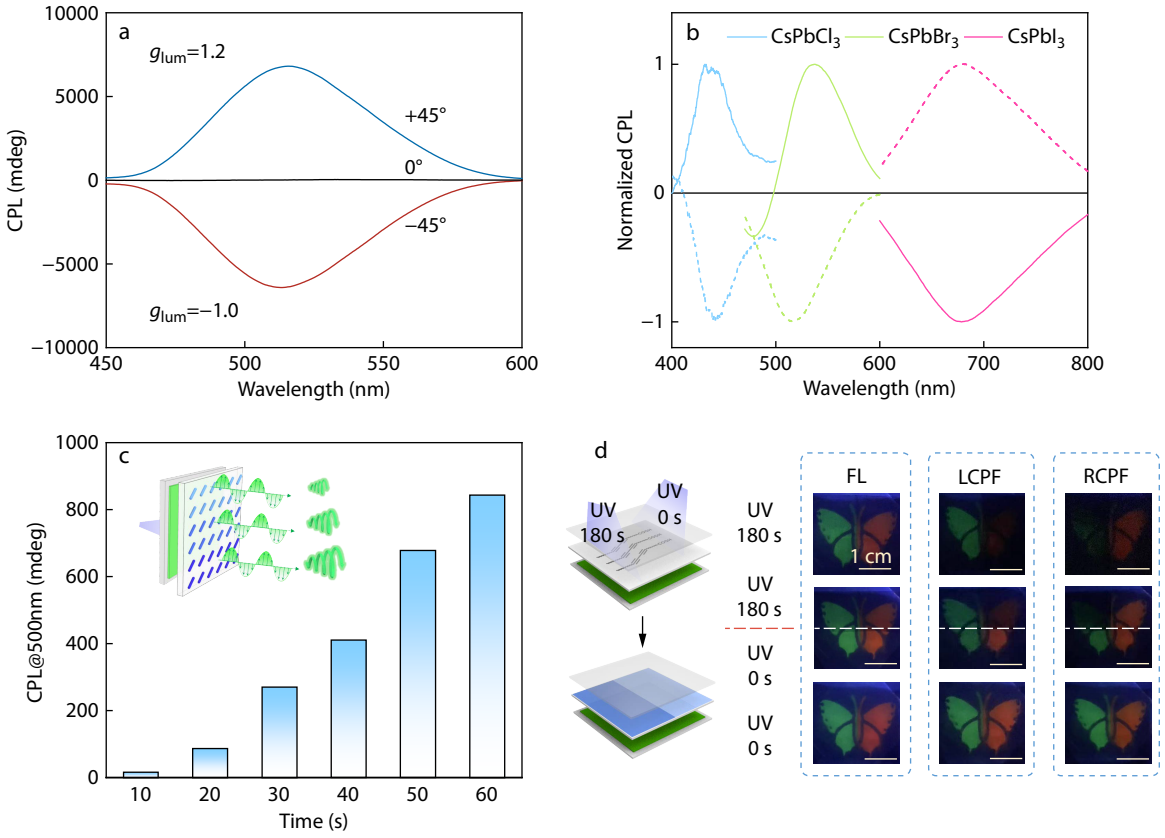

Fig. 2 (a) CPL signals obtained at $CsPbBr_3$/PDA/PVA composite film with twist angle of 0°, +45°, and –45°; (b) CPL responses of three perovskite nanocrystals with different emission wavelengths ($CsPbCl_3$, $CsPbBr_3$, $CsPbI_3$). Solid lines correspond to +45° stacking, and dashed lines correspond to –45° stacking; (c) CPL signal intensity at 500 nm for the green-emitting perovskite composite film as a function of PDA polymerization time; (d) Photographs of the red-green dual-color perovskite patterns under direct observation (FL), left-handed circular polarization filtering (LCPF), and right-handed circular polarization filtering (RCPF) at different stages: initial state (UV 0 s), partial polymerization (UV 180 s), and full polymerization (UV 180 s).

was enhanced with an increased stacking number of PDA layers at a constant DC value (Fig. S11b in ESI). In distinct contrast, as the thickness of the PVA layer increased, the CPL signal underwent two chiral reversals, changing sequentially from negative to positive and then back to negative (Fig. S11c in ESI).[43] On this basis, a hybrid fluorescent film with a visual butterfly pattern was fabricated to validate the material's potential for dynamic anti-counterfeiting applications. Specifically, the left and right wings of the butterfly pattern were printed using the $CsPbBr_3$ and $CsPbI_3$ nanocrystals, respe ctively. As shown in Fig. 2(d), the unpolymerized perovskite/PDA/PVA composite film exhibited negligible CPL signals in the absence of UV irradiation (0 s). Under unpolarized UV excitation, the butterfly pattern displayed distinct green and red wings observable by the naked eye, with no obvious intensity difference when viewed through left- or right-handed circular polarization filtering (L- or R-CPF). After UV irradiation for 180 s, the partially polymerized upper region of the pattern presented obvious intensity asymmetries in the left-handed circular polarization filtering (LCPF), and right-handed circular polarization filtering (RCPF) observations, while the unpolymerized lower region remained unchanged. Upon subsequent polymerization of whole films, selective observation under LCPF and RCPF enabled the independent display of green and red wings, respectively (Fig. 2d). These results demonstrate the achievement of dynamic CPL switching and pattern encryption based on the photopolymerization behavior of the PDA.

Modulation of Circularly Polarized Luminescence (CPL)

Dynamic modulation of emission wavelengths is highly desirable for constructing high-performance multi-level optical encryption systems. Herein, we realize a wide-range modulation of the fluorescence emission wavelength through anion exchange of $CsPbX_3$ perovskite nanocrystals. Taking the $CsPbBr_3$/PDA/PVA composite film as a typical example, the fluorescence emission of $CsPbBr_3$ exhibited a blue shift after the controlled HCl treatment. The CPL signal of the composite film evolved from nearly zero to the maximum positive CPL response. In contrast, immersion in the HI solution induced a redshift of the emission peak, accompanied by a gradual transition of the CPL signal toward the maximum negative value (Fig. 3a). The optical photographs captured under UV excitation (Fig. S12 in ESI) were highly consistent with the corresponding CPL and fluorescence spectral results (Fig. S13 in ESI), demonstrating a reliable platform for exploring wavelength-dependent chiroptical responses.

PDA is a distinctive conjugated polymer with environmentally responsive optical properties. Upon heating, PDA

https://doi.org/10.1007/s10118-026-3821-4

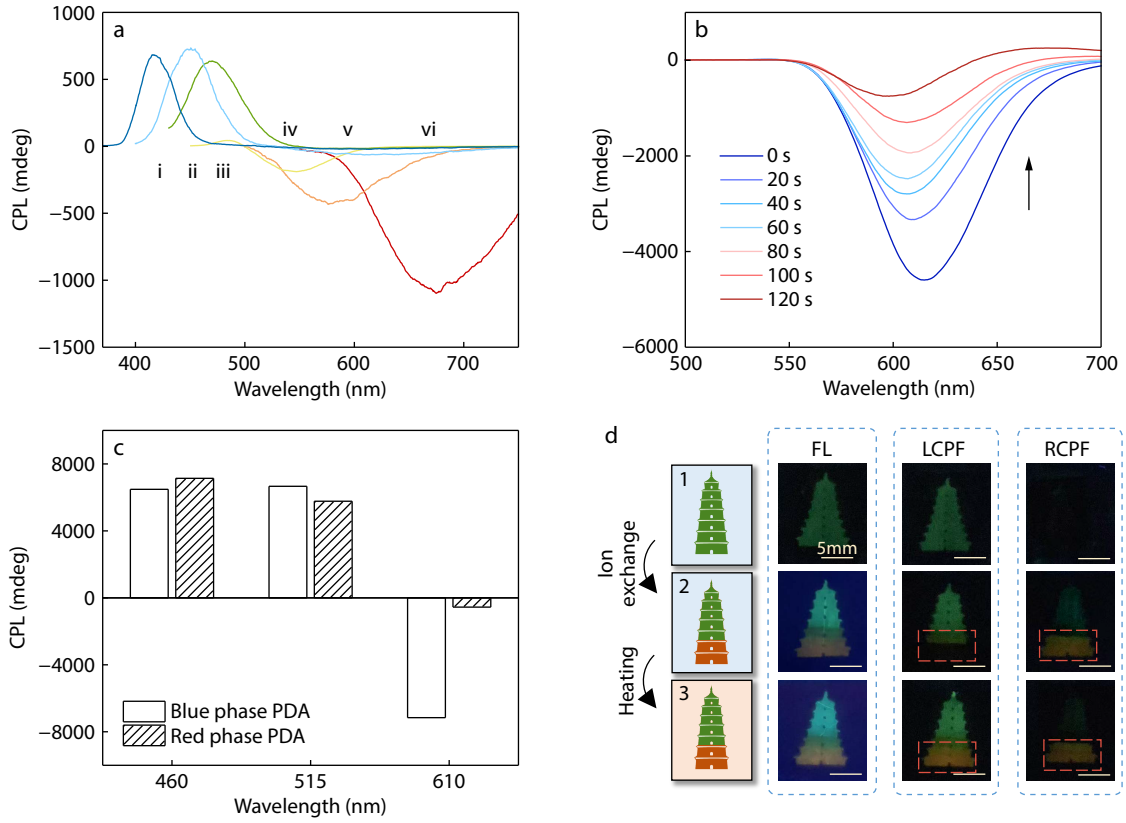

Fig. 3 (a) CPL spectra of perovskite/PDA/PVA composite films during anion exchange treatment: HCl treatment for (i) 20 min, (ii) 10 min, (iii) initial state, HI treatment for (iv) 10 min, (v) 20 min, (vi) 30 min; (b) Upon prolonged heating at 80 °C, the PDA layer in $CsPbI_3$/PDA/PVA composite films gradually undergoes phase transition into the red phase, accompanied by sustained attenuation of CPL signals; (c) Variations in maximum CPL intensity of perovskite nanocrystals with three distinct emission peaks during the blue-to-red phase transition of PDA; (d) After regional selective anion exchange and thermal treatment, the tower-patterned composite film presents fluorescence images under direct observation, LCPF and RCPF. Scale bar: 5 mm.

changes from a blue phase to a red one that exhibits characteristic absorption peaks at 550 and 505 nm. The PDA films coated on the glass substrates were placed on a heating stage, and their UV-Vis absorption spectra were recorded every 20 s until a complete shift of the absorption peak was observed (Fig. S14 in ESI). After cooling, the absorption spectra of the PDA films were re-measured, and no recovery of the original signal was detected. Under external stimuli, such as thermal treatment at 80 °C for 10 min, polymerized blue-phase PDA underwent a blue-to-red thermochromic phase transition of its molecular chains, accompanied by macroscopic color changes and characteristic red shifts in its absorption (Fig. S14 in ESI) and CD spectra (Fig. S15 in ESI). Importantly, this phase transition induced distinct variations in the CPL responses of the three-perovskite nanocrystal composite films. Specifically, the CPL intensity of the $CsPbI_3$/PDA/PVA composite film was steadily and continuously tuned from 5000 to nearly zero, which originated from the pronounced attenuation of the CD signal during the PDA phase-transition process (Fig. 3b). In contrast, the CPL signal intensities of $CsPbCl_3$/PDA/PVA and $CsPbBr_3$/PDA/PVA composite films remained nearly unaltered (Fig. 3c).

Based on these findings, we fabricated chiral optical composite films with tower-shaped fluorescent patterns. As shown in Fig. 3(d), the pristine composite film exhibited uniform green fluorescence under unpolarized ultraviolet excitation. After regionally selective anion exchange *via* localized HI treatment, the $CsPbBr_3$ component in the lower half of the patterned structure was transformed into $CsPbI_3$ and emitted red fluorescence, establishing a dual-color emission profile. At this stage, owing to the opposite CPL handedness at different wavelengths, only the upper tower region was observable under the LCPF, whereas only the lower region could be detected under the RCPF. After thermal treatment at 80 °C for 10 min, PDA underwent a typical blue-to-red phase transition, which induced stepwise variations in the observed fluorescence patterns under LCPF and RCPF. Specifically, the red fluorescent region showed negligible changes under both LCPF and RCPF (Fig. 3d), whereas the green fluorescent region exhibited distinct switching behavior in fluorescence intensity.

Multi-mode information encoding has attracted tremendous research interest owing to its remarkable capability to improve information-encoding capacity and enhance data security. To explore the practical applicability of composite films in high-level anti-counterfeiting, three-colored perovskite materials were fabricated in a 4×4 pixel array, forming a QR code pattern (Fig. 4). Each pixel unit corresponds to an independent segment of the complete QR code and displays a unique color and optical activity (Fig. S16 in ESI). The handedness of the CPL could be effectively modulated by

https://doi.org/10.1007/s10118-026-3821-4

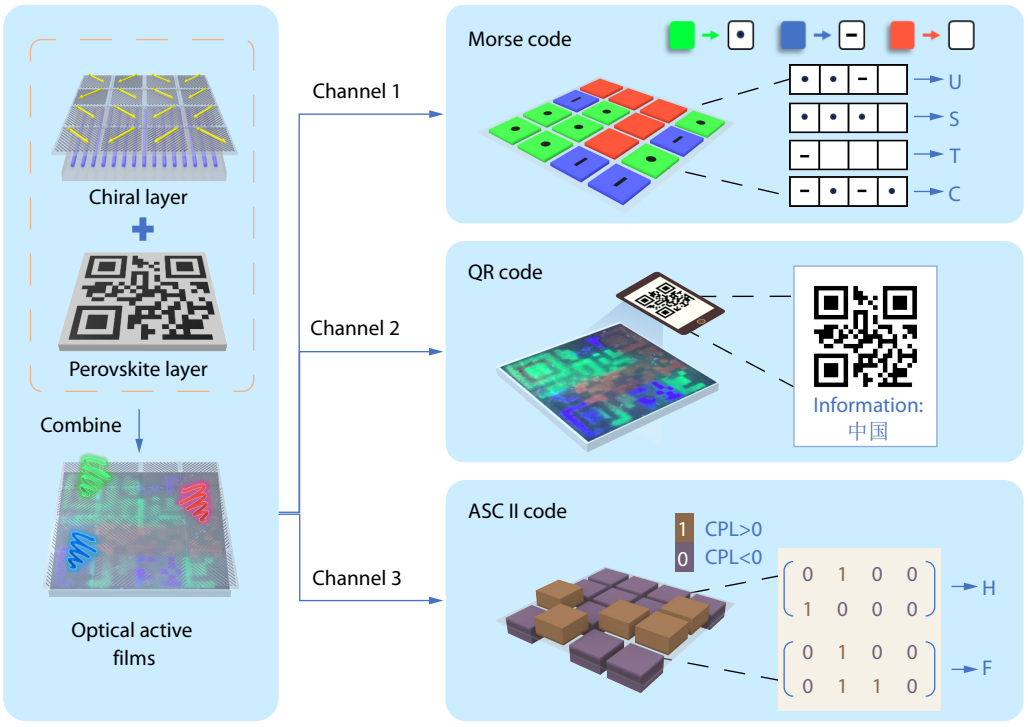

Fig. 4 Multimodal anti-counterfeiting strategy based on chiral fluorescent composite films. A multi-level information encryption platform is fabricated by integrating chiral PVA layers with perovskite functional layers, which endows the system with three mutually independent decryption channels. Channel 1 realizes information decryption of "USTC" *via* fluorescent Morse code under UV light excitation. Channel 2 relies on fluorescent QR code patterns, where the encrypted text "China" can be acquired through smartphone scanning. For Channel 3, American Standard Code for Information Interchange (ASCII) encryption is achieved based on CPL signals. Specifically, positive and negative CPL signals are defined as binary "1" and "0", respectively, enabling the decryption of the encrypted information "HF".

tuning the twist angles of the oriented PVA layer. Three independent information encryption channels were constructed based on the unpolarized UV-excited fluorescence emission, macroscopic QR code pattern, and CPL signals, defined as channels 1, 2, and 3, respectively. In Channel 1, green, blue, and red fluorescence emissions were assigned to the Morse code symbols "•", "-" and a blank space, enabling the top-to-bottom decryption of the coded text string "USTC" (Fig. S17 in ESI). In Channel 2, the screen-printed QR code pattern was visually observable by the naked eye and easily recognizable *via* smartphone scanning, which allowed the extraction of the encrypted message "China" (Fig. S18 in ESI). In Channel 3, a binary encryption algorithm compliant with the American Standard Code for Information Interchange (ASCII) was established, where CPL values greater than 0 were defined as binary "1" and those less than 0 as binary "0." Encrypted information "HF" was successfully decoded through regional CPL signal analysis (Fig. S19 in ESI). This triple-channel multiplexing strategy exhibited distinct superiority over conventional anti-counterfeiting technologies in three key respects. First, the integration of three diverse authentication approaches establishes a multi-level security system that is highly resistant to replication and counterfeiting. Second, all channels operate independently with no mutual signal interference, realizing high-density information storage within a single anti-counterfeiting tag. Third, the fluorescence emission, patterned morphology, and CPL signals were programmable, offering excellent flexibility for customized information encryption. Collectively, these results demonstrate that the combination of patterned fluorescence and chiral optical modulation is a robust and promising strategy for the development of next-generation high-security anti-counterfeiting labels.

Multi-level Information Encryption

The development of stimulus-responsive materials with multi-level encryption functionality is a robust strategy for advancing information security. In this study, two mutually independent signal dimensions (emission wavelength and CPL handedness) were integrated to improve information storage density and strengthen encryption performance. Specifically, the FL channel enables dynamic modulation of the emission peak of perovskite nanocrystals *via* anion exchange, whereas the CPL channel can be precisely tuned through the thermally induced phase transition of the PDA layer. The innovative integration of these two independent channels realizes a two-step decryption procedure for an accurate final information output, as illustrated in Fig. 5.

First, a customized coding matrix was established, in which the distinct fluorescence emissions of the two-dimensional pixel array were defined as specific ASCII symbols. In this system, green fluorescence was designated as the symbol "0," whereas red fluorescence corresponded to "1" (Fig. S20 in ESI). Furthermore, all the pixel arrays exhibited intrinsic CPL properties. Extensive CPL spectroscopic tests were conducted to characterize the CPL signals of each pixel array, and three signal states, namely positive, negative, and zero responses, were observed. Specifically, pixel arrays with posi-

https://doi.org/10.1007/s10118-026-3821-4

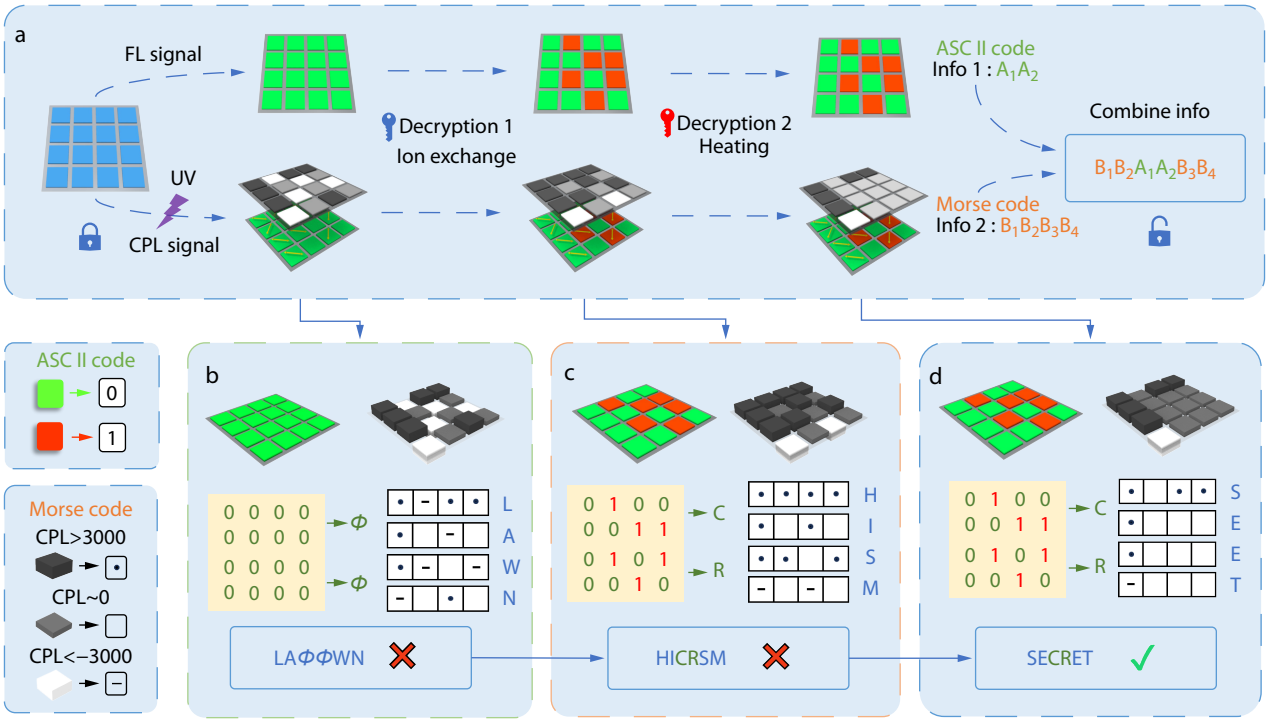

Fig. 5 Schematic illustration of composite film pixel arrays for information storage and encryption. The two-dimensional pixel array-based encryption system demonstrates information transition and corresponding decoded results upon two sequential decryption steps: anion exchange and heat treatment. (a) The process diagram of two-step decryption; (b) Information of the initial camouflaged state; (c) Information after the first-step decryption; (d) Information after the second-step decryption.

tive, negative, and zero CPL signals are marked in black, white, and gray, respectively, to construct a complete CPL information pattern. Moreover, CPL signals were classified based on magnitude thresholds as follows: CPL > 3000 mdeg, < −3000 mdeg, and close to zero were assigned to the Morse code symbols "•", "-," and a blank space.

Initially, all pixel arrays exhibited green fluorescence, corresponding to decoded fluorescence information of "ΦΦ" and CPL-decoded information of "LAWN" (Fig. S21 in ESI). The superposition of the two sets of information yielded the combined output "LAΦΦWN" (Fig. 5). Following the anion exchange treatment, the partial pixel arrays switched to red fluorescence emission, as illustrated in Fig. 3. The variation in the emission wavelength further induced a sign inversion of the corresponding CPL signals (Fig. S22 in ESI), generating decoded information of "HICRSM" (Fig. 5). Crucially, this information was camouflaged data that served to prevent unauthorized interception. Subsequent thermal treatment triggered a phase transition of the PDA layer from blue to red. This structural evolution substantially reduced the CPL signal intensity of the red fluorescence to nearly zero, while the CPL signals of the green fluorescence remained nearly unchanged (Fig. S23 in ESI). Ultimately, the authentic target information "SECRET" was successfully decoded using this two-step modulation strategy (Fig. 5). In this multi-level encryption system, each external stimulus serves as an independent encryption key, and the target information can only be decrypted *via* the synergistic effect of the dual keys. The as-fabricated composite film pixel array exhibited superior information storage and encoding performance, enabling the realization of high-security multi-level encryption. This study presents great application potential for the reliable protection of confidential and authentic information.

CONCLUSIONS

In conclusion, we rationally designed and successfully fabricated a high-performance CPL-active optical system with high dissymmetry factor, orthogonal stimulus responsiveness, and dynamic tunability. The architecture comprises a luminescent perovskite film integrated onto a twisted-stacking anisotropic PDA/PVA heterostructure, wherein the underlying perovskite film yields tunable photoluminescence, whereas the anisotropic PDA layer and PVA phase retarder serve as polarization-selective modulation components to convert unpolarized emission into circularly polarized luminescence. Based on this hierarchical structure, a multimodal information encryption strategy was successfully demonstrated, which enabled independent modulation of fluorescence emission, optical patterns, and CPL signals. Notably, the composite film integrates a dual-key and multistage decryption mechanism driven by two orthogonal external stimuli, namely halogen anion exchange and thermal treatment, which substantially improves the information storage density and security level of the encryption system. The proposed composite film and triple-channel multiplexing strategy realizes the fully independent regulation of three optical signal channels and effectively eliminates inter-channel crosstalk, whose dual-stimulus orthogonal response mechanism imparts excellent security and programmability to the information en-

https://doi.org/10.1007/s10118-026-3821-4

cryption system.

Conflict of Interests

The authors declare no interest conflict.

Electronic Supplementary Information

Electronic supplementary information (ESI) is available free of charge in the online version of this article at http://doi.org/10.1007/s10118-026-3821-4.

Data Availability Statement

Data supporting the findings of this study are available in the supplementary material of this article, and can be obtained from the author for reasonable reasons. The author's contact information: gangzou@ustc.edu.cn, zhl1992@ustc.edu.cn, yfxie@ustc.edu.cn.

ACKNOWLEDGMENTS

This work was financially supported by the National Natural Science Foundation of China (No. 52373122), Young Scientists Fund of the National Natural Science Foundation of China (Nos. 52503119 and 52403119), Open Research Fund of Suzhou Laboratory (No. SZLAB-1508-2024-ZD017), Youth Project of the Provincial Natural Science Foundation of Anhui (No. 2408085QB041), China Postdoctoral Science Foundation (No. 2024M753108), and Anhui Estone Materials Technology Co., Ltd. This work was partially carried out at the University of Science and Technology of China's Center for Micro-and Nanoscale Research and Fabrication and the Center for Physical Science, University of Science and Technology of China.

REFERENCES

1 Shen, Y.; Le, X.; Wu, Y.; Chen, T. Stimulus-responsive polymer materials toward multi-mode and multi-level information anti-counterfeiting: recent advances and future challenges. *Chem. Soc. Rev.* **2024**, *53*, 606–623.
2 Liu, D.; Zhao, J.; Zhao, X.; Shi, S.; Li, S.; Wang, Y.; Song, Q.; Cheng, X.; Zhang, W. Chiral polymer micro/nano-objects: evolving preparation strategies in heterogeneous polymerization. *Sci. China Chem.* **2025**, *68*, 1779–1793.
3 He, Z.; Fang, X.; Yuan, X.; Zhang, G.; Zhang, W. Chiral supramolecular materials based on azobenzene self-assembly systems: from regulated helix structures to chiral functions. *Sci. China Mater.* **2026**, *69*, 2427–2447.
4 Zijlstra, P.; Chon, J. W. M.; Gu, M. Five-dimensional optical recording mediated by surface plasmons in gold nanorods. *Nature* **2009**, *459*, 410–413.
5 Wang, Q.; Lin, B.; Chen, M.; Zhao, C.; Tian, H.; Qu, D. H. A dynamic assembly-induced emissive system for advanced information encryption with time-dependent security. *Nat. Commun.* **2022**, *13*, 4185.

Graphical Abstract

Stimuli-responsive Perovskite Hybrid Films towards Multi-mode and Dual-key Multi-level Information Encryption

Cong-Yang Ye, Ze-Yu Feng, Jia-He Li, Di Wang, Xiang-Xiang Xu, Yi-Fan Xie, Hong-Li Zhang, and Gang Zou

University of Science and Technology of China

Twisted-stacking perovskite/polydiacetylene/poly(vinyl alcohol) hybrid films realize orthogonal modulation of pattern, fluorescence and high-glum CPL. Dual stimuli (halogen exchange/heating) serve as independent keys for multi-level hierarchical information encryption with zero inter-channel crosstalk.

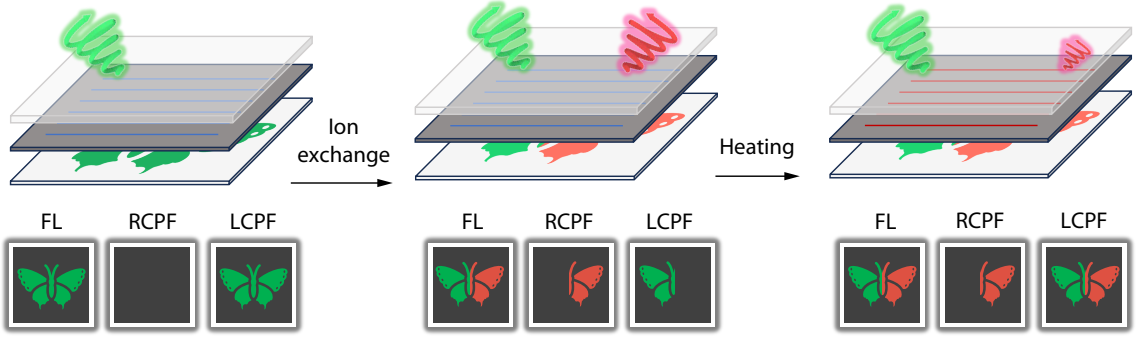

Chinese J. Polym. Sci. 2026 *https://doi.org/10.1007/s10118-026-3821-4*

6 Peng, H.; Bi, S.; Ni, M.; Xie, X.; Liao, Y.; Zhou, X.; Xue, Z.; Zhu, J.; Wei, Y.; Bowman, C. N.; Mai, Y.-W. Monochromatic visible light "photoinitibitor": Janus-faced initiation and inhibition for storage of colored 3D images. *J. Am. Chem. Soc.* **2014**, *136*, 8855–8858.

7 Ji, X.; Chen, W.; Long, L.; Huang, F.; Sessler, J. L. Double layer 3D codes: fluorescent supramolecular polymeric gels allowing direct recognition of the chloride anion using a smart phone. *Chem. Sci.* **2018**, *9*, 7746–7752.

8 Bin Kim, J.; Chae, C.; Han, S. H.; Lee, S. Y.; Kim, S. H. Direct writing of customized structural-color graphics with colloidal photonic inks. *Sci. Adv.* **2021**, *7*, eabj8780.

9 Xie, H.; Wang, J.; Lou, Z.; Hu, L.; Segawa, S.; Kang, X.; Wu, W.; Luo, Z.; Kwok, R. T. K.; Lam, J. W. Y.; Zhang, J.; Tang, B. Z. Mechanochemical fabrication of full-color luminescent materials from aggregation-induced emission prefluorophores for information storage and encryption. *J. Am. Chem. Soc.* **2024**, *146*, 18350–18359.

10 Zhang, F.; Li, Q.; Wang, C.; Wang, D.; Song, M.; Li, Z.; Xue, X.; Zhang, G.; Qing, G. Multimodal, convertible, and chiral optical films for anti-counterfeiting labels. *Adv. Funct. Mater.* **2022**, *32*, 2204487.

11 Guo, Q.; Zhang, M.; Tong, Z.; Zhao, S.; Zhou, Y.; Wang, Y.; Jin, S.; Zhang, J.; Yao, H. B.; Zhu, M.; Zhuang, T. Multimodal-responsive circularly polarized luminescence security materials. *J. Am. Chem. Soc.* **2023**, *145*, 4246–4253.

12 Javidi, B.; Carnicer, A.; Yamaguchi, M.; Nomura, T.; Pérez-Cabré, E.; Millán, M. S.; Nishchal, N. K.; Torroba, R.; Barrera, J. F.; He, W.; Peng, X.; Stern, A.; Rivenson, Y.; Alfalou, A.; Brosseau, C.; Guo, C.; Sheridan, J. T.; Situ, G.; Naruse, M.; Matsumoto, T.; Juvells, I.; Tajahuerce, E.; Lancis, J.; Chen, W.; Chen, X.; Pinkse, P. W. H.; Mosk, A. P.; Markman, A. Roadmap on optical security. *J. Opt.* **2016**, *18*, 083001.

13 Liu, S.; Liu, X.; Yuan, J.; Bao, J. Multidimensional information encryption and storage: when the input is light. *Research* **2021**, *2021*, 7897849.

14 Wang, H.; Jin, L.; Mo, W.; Hong, W. Dynamic encryption enabled by circularly polarized carbon dot-based afterglow composites featuring hierarchical tri-mode thermochromic emission. *Chem. Eng. J.* **2025**, *512*, 162427.

15 Xiang, Y.; Zhong, L.; Long, Y.; Liu, S.; Cheng, Z.; Rao, S.; Hong, J.; Lei, B.; Suo, H.; Zhang, J.; Zhou, L.; Wang, F.; Wu, M. Deciphering defect-mediated anti-thermal quenching multimodal luminescence for information encryption. *Adv. Mater.* **2026**, *38*, e15825.

16 Liu, Z.; Chen, Z.; Yang, S.; Jia, H.; Wei, J. Dual-mode multicolor display based on structural and fluorescent color CdS photonic crystal hydrogel. *Langmuir* **2024**, *40*, 12767–12777.

17 Zhao, Y.; Zhao, X.; Li, M. D.; Li, Z.-A.; Peng, H.; Xie, X. Crosstalk-free patterning of cooperative-thermoresponse images by the synergy of the AIEgen with the liquid crystal. *Angew. Chem. Int. Ed.* **2020**, *59*, 10066–10072.

18 Baiheti, Y.; Yang, P.; Xie, Y.; Gan, L.; Liu, X.; Wen, L.; Feng, Z.; Chu, X.; Zhang, H.; Chen, X.; Zou, G. Biomimetic multicolored polyfluorene circularly polarized luminescence micro-patterns towards multilevel encryption. *Chin. J. Chem.* **2025**, *43*, 3388–3396.

19 Gong, Z. L.; Zhu, X.; Zhou, Z.; Zhang, S. W.; Yang, D.; Zhao, B.; Zhang, Y. P.; Deng, J.; Cheng, Y.; Zheng, Y. X.; Zang, S. Q.; Kuang, H.; Duan, P.; Yuan, M.; Chen, C. F.; Zhao, Y. S.; Zhong, Y. W.; Tang, B. Z.; Liu, M. Frontiers in circularly polarized luminescence: molecular design, self-assembly, nanomaterials, and applications. *Sci. China Chem.* **2021**, *64*, 2060–2104.

20 Lin, S.; Tang, Y.; Kang, W.; Bisoyi, H. K.; Guo, J.; Li, Q. Photo-triggered full-color circularly polarized luminescence based on photonic capsules for multilevel information encryption. *Nat. Commun.* **2023**, *14*, 3005.

21 Feng, Z.; Li, J.; Yang, P.; Xu, X.; Wang, D.; Li, J.; Zhang, C.; Li, J.; Zhang, H.; Zou, G.; Chen, X. Dynamic multimodal information encryption combining programmable structural coloration and switchable circularly polarized luminescence. *Nat. Commun.* **2025**, *16*, 2264.

22 Qin, J.; Yao, X.; Wang, S.; Lu, Y.; Yang, D.; Zhong, Z.; Hu, S.; Yang, Z.; Cao, H.; He, W.; Zhao, Y.; Wang, D. Synergistic chiral diffusion and dual-mode luminescence in flexible polymer-stabilized cholesteric liquid crystal films for multistate anti-counterfeiting and dynamic information encryption. *ACS Appl. Mater. Interfaces* **2026**, *18*, 23648–23659.

23 Wang, T.; Li, X.; Zhang, Y.; Ma, H.; Sun, Y. Cholesteric liquid crystal network composite film with structure, dual-band responsive luminescent color for multiple anti-counterfeiting and information encryption. *ACS Appl. Mater. Interfaces* **2024**, *16*, 68498–68505.

24 Shi, Z.; Zheng, Z.; Wang, H.; Xu, X.; Li, X.; Zhang, Q.; Zhao, Q.; Shi, J.; Xu, M.; Zhang, F.; Guo, Y. Multi-dimensional multiplexing cascaded liquid crystal elements for compartmentalized optical encryption. *Laser Photonics Rev.* **2026**, *20*, e03039.

25 Sun, R.; Liu, S. J.; Zhang, Y. H.; Xu, P. H.; Zhu, L.; Zhu, D.; Chen, W.; Wang, Y. M.; Ding, S. H.; Ge, S. J.; Chen, P.; Wei, B. Y.; Zhao, J. L.; Lu, Y. Q. Touch-driven bi-chiral superstructures for nested encryption of multiplexed optical information. *Adv. Mater.* **2026**, *38*, e13318.

26 Zhang, J.; Shen, H.; Liu, X.; Yang, X.; Broman, S. L.; Wang, H.; Li, Q.; Lam, J. W. Y.; Zhang, H.; Cacciarini, M.; Nielsen, M. B.; Tang, B.-Z. A dihydroazulene-based photofluorochromic AIE system for rewritable 4D information encryption. *Angew. Chem. Int. Ed.* **2022**, *61*, e202208460.

27 Kim, J. J.; Kim, M. S.; Lee, G. J. Multi-level optical physical unclonable function based on random surface scattering for hierarchical cryptographic protocols. *Adv. Sci.* **2025**, *12*, e12317.

28 Huang, X.; Liang, Z.; Yang, X.; Piao, M.; Huang, Z.; Zhang, Z. Multilevel anti-counterfeiting barcode with enhanced information encryption based on stimulus-responsive digital polymers. *ACS Appl. Mater. Interfaces* **2024**, *16*, 43075–43082.

29 Cucuiet, T. A.; Vargas Jentzsch, A.; Picini, F.; Maaloum, M.; Raffy, G.; Moulin, E.; Bassani, D. M.; Giuseppone, N. Inverting the circularly polarized luminescence handedness of chiral supramolecular polymers using temperature. *Angew. Chem. Int. Ed.* **2025**, *64*, e202516824.

30 Hu, Y.; Huang, Z.; Willner, I.; Ma, X. Multicolor circularly polarized luminescence of a single-component system revealing multiple information encryption. *CCS Chem.* **2024**, *6*, 518–527.

31 Chen, H.; Hu, H.; Sun, B.; Zhao, H.; Qie, Y.; Luo, Z.; Pan, Y.; Chen, W.; Lin, L.; Yang, K.; Guo, T.; Li, F. Dynamic anti-counterfeiting labels with enhanced multi-level information encryption. *ACS Appl. Mater. Interfaces* **2023**, *15*, 2104–2111.

32 Lan, X.; Xu, S.; Sun, C.; Zheng, Y.; Wang, B.; Shan, G.; Bao, Y.; Yu, C.; Pan, P. Multi-level information encryption/decryption of fluorescent hydrogels based on spatially programmed crystal phases. *Small* **2023**, *19*, 2205960.

33 Shi, J.; Wang, Z.; Jia, N.; Wang, M.; Xu, Y.; Li, X.; Shao, J. Patterned lead-free double perovskite/polymer fluorescent piezoelectric composite films for advanced anti-counterfeiting. *Adv. Sci.* **2025**, *12*, 2409692.

34 Huo, S.; Duan, P.; Jiao, T.; Peng, Q.; Liu, M. Self-assembled luminescent quantum dots to generate full-color and white circularly polarized light. *Angew. Chem. Int. Ed.* **2017**, *56*, 12174–12178.

35 Wang, Y.; Song, M.-S.; Zhao, J.; Li, Z.; Wang, T.; Wang, H.; Wang, H.-Y.; Wang, Y. Chiral perovskite heterostructure films of $CsPbBr_3$ quantum dots and 2D chiral perovskite with circularly polarized

luminescence performance and energy transfer. *ACS Nano* **2024**, *18*, 22334−22343.
36 Khorloo, M.; Yu, X.; Cheng, Y.; Zhang, H.; Yu, S.; Lam, J. W. Y.; Zhu, M.; Tang, B. Z. Enantiomeric switching of the circularly polarized luminescence processes in a hierarchical biomimetic system by film tilting. *ACS Nano* **2021**, *15*, 1397−1406.
37 Zhou, B.; Cao, L. H.; Huang, M. F.; Yang, Y.; Qi, S.; Cao, X. J.; Chen, X.-Y. Temperature and solvent dual switch photochromic chiral ionic hydrogen-bonded organic framework for circularly polarized luminescence and advanced encryption. *Angew. Chem. Int. Ed.* **2025**, *64*, e202504645.
38 Liang, D.; Peng, F.; Du, Q.; Zhao, Y.; Ma, W. Gadolinium and europium doped chiral perovskite films with magnetic circular dichroism and circularly polarized luminescence for information encryption applications. *Angew. Chem. Int. Ed.* **2025**, *64*, e202510754.
39 Fu, K.; Qu, D. H.; Liu, G. Reversible circularly polarized luminescence inversion and emission color switching in photo-modulated supramolecular polymer for multi-modal information encryption. *J. Am. Chem. Soc.* **2024**, *146*, 33832−33844.
40 Zhang, H.; Zou, G. Artificial intelligence-enabled chiral functional materials design. *Sci. China Mater.* **2026**, *69*, 2343−2357.
41 Lv, J.; Hou, K.; Ding, D.; Wang, D.; Han, B.; Gao, X.; Zhao, M.; Shi, L.; Guo, J.; Zheng, Y.; Zhang, X.; Lu, C.; Huang, L.; Huang, W.; Tang, Z. Gold nanowire chiral ultrathin films with ultrastrong and broadband optical activity. *Angew. Chem. Int. Ed.* **2017**, *56*, 5055−5060.
42 Xie, Y.; Feng, S.; Deng, L.; Cai, A.; Gan, L.; Jiang, Z.; Yang, P.; Ye, G.; Liu, Z.; Wen, L.; Zhu, Q.; Zhang, W.; Zhang, Z.; Li, J.; Feng, Z.; Zhang, C.; Du, W.; Xu, L.; Jiang, J.; Chen, X.; Zou, G. Inverse design of chiral functional films by a robotic AI-guided system. *Nat. Commun.* **2023**, *14*, 6177.
43 Wen, L.; Yang, P.; Mo, S.; Wang, D.; Sheng, N.; Xu, X.; Zhang, H.; Lu, H.; Zou, G. Multi-responsive circularly polarized luminescence micro-patterns with high figure of merit towards multi-dimensional data encoding. *Chem. Eng. J.* **2025**, *505*, 159821.

https://doi.org/10.1007/s10118-026-3821-4